13th Australasian Fluid Mechanics Conference
Monash University, Melbourne, Australia
13-18 December 1998

MIXING BY NATURAL CONVECTION

A. Mark JELLINEK, Ross C. KERR and Ross W. GRIFFITHS

Research School of Earth Sciences,
The Australian National University, Canberra, AUSTRALIA

ABSTRACT

An extensive series of laboratory experiments is used to quantify the circumstances under which fluids can be mixed by natural convection at high Rayleigh number. A compositionally buoyant fluid was injected at a fixed rate into an overlying layer of ambient fluid from a planar, horizontally uniform source. The nature of the resulting compositional convection was found to depend on two key dimensionless parameters: a Reynolds number *Re* and the ratio *U* of the ambient fluid viscosity to the input fluid viscosity. Increasing the Reynolds number corresponded to increasing the vigour of the convection, while the viscosity ratio was found to determine the spacing between plumes and whether buoyant fluid rose as sheets ($U < 1$) or axisymmetric plumes ($U > 1$). From measurements of the final density profile in the fluid after the experiments, we quantified the extent to which buoyant liquid was mixed in terms of a thermodynamic mixing efficiency *E*. The mixing efficiency was found to be high ($E > 0.9$) when either the Reynolds number was large ($Re > 100$) or the viscosity ratio was small ($U < 0.2$), and found to be low ($E < 0.1$) when both $Re < 1$ and $U > 200$. The amount of mixing was related to whether ascending plumes generated a large-scale circulation in the ambient fluid.

INTRODUCTION

In a very wide range of geological, geophysical and industrial situations, natural convection is produced by the continuous release of buoyant fluid from a boundary into an overlying layer of denser fluid. In these circumstances, a fundamental question to ask is: will the convection lead to mixing of the two fluids?

In this paper we summarize a series of laboratory experiments (Jellinek, Kerr and Griffiths, 1998) that quantify the mixing efficiency as a function of the primary dimensionless parameters that control the convection. All of our experiments were conducted at large flux Rayleigh numbers and so velocity fields were always unsteady and motions were complex. We find that the extent of mixing is determined primarily by whether ascending plumes are able to generate a large-scale overturning circulation, and that the nature of the circulation depends on a Reynolds number and a viscosity ratio.

DIMENSIONLESS PARAMETERS

Consider the release of a light (input) fluid of density ρ_i, and kinematic viscosity ν_i, at a fixed volume flux per unit area V_i, into a stagnant, comparatively dense overlying fluid of depth *H*, density ρ_a, and kinematic viscosity ν_a (figure 1).

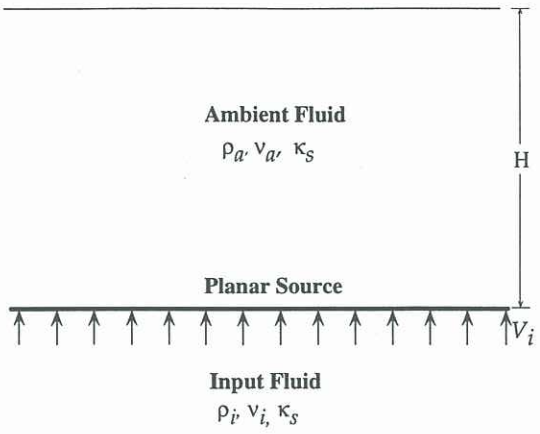

Figure 1 : Definition sketch of our mixing experiments. A compositionally buoyant fluid is input at a fixed velocity from a planar boundary into an overlying ambient fluid layer.

The two fluids have different compositions, but are assumed to have a uniform compositional diffusivity κ_s. The flow can be defined in terms of five variables: the weight deficiency per unit time and unit area (buoyancy flux) supplied from the boundary $B = gV_i(\rho_a - \rho_i)/\rho_a$ (where *g* is the gravitational acceleration), ν_i, ν_a, κ_s and *H*. From these five parameters we form three dimensionless numbers, which are the compositional flux Rayleigh number,

$$Ra_f = \frac{g(\rho_a - \rho_i)V_i H^4}{\rho_a \nu_a \kappa_s^2} = \frac{BH^4}{\nu_a \kappa_s^2}, \qquad (1)$$

the Schmidt number

$$Sc = \frac{\nu_a}{\kappa_s}, \qquad (2)$$

and the viscosity ratio

$$U = \frac{\nu_a}{\nu_i}. \qquad (3)$$

The flux Rayleigh number relates to the relative proportions of vertical advective and diffusive mass transfer over the imposed length scale *H*. When $Ra_f >> 10^3$, mass transfer away from the source of buoyancy is by advection. In all of our experiments, the flux Rayleigh numbers were very large ($Ra_f > 10^{11}$), so that the resulting convection was highly unsteady with

very thin (compared to the depth H) compositional boundary layers at the boundary and around rising plumes.

The Schmidt number provides a comparison of the thicknesses of these chemical and viscous boundary layers. In all of our experiments $Sc > 800$, so that for a given time scale, momentum diffuses much more widely through the ambient fluid than composition. The viscosity ratio U is a measure of the relative importance of viscous stresses in the two fluids, and has an influence on the spacing and structure of the buoyant plumes (Whitehead and Luther, 1975).

In order to understand explicitly the relative significance of inertial and viscous forces it is useful to define an internal parameter called the Reynolds number

$$Re = \frac{Wd}{\nu_a}, \tag{4}$$

where W and d are convective velocity and length scales. The most relevant length scale is H since this is the only externally-imposed scale for the convective motions. We choose a velocity scale defined by Kraichnan (1962)

$$W \sim B^{\frac{1}{3}} H^{\frac{1}{3}}. \tag{5}$$

The resulting Reynolds number can be written in terms of the externally-controlled flux Rayleigh and Schmidt numbers,

$$Re \sim Ra_f^{\frac{1}{3}} Sc^{\frac{-2}{3}}, \tag{6}$$

so that the system is defined by a new set of three dimensionless parameters, which are Re, Sc and U.

EXPERIMENTAL TECHNIQUES

To quantify the extent of mixing in a large region of Re – U parameter space, we used two experimental designs. In the first, the buoyancy flux was obtained by melting, as done by Kerr (1994). We used this method to explore mixing when $Re > 20$ and $U < 5$. In the second design, we pumped fluid through a porous plate into the base of a denser ambient fluid layer. A variety of input and ambient fluids were used (c.f. Jellinek, Kerr and Griffiths, 1998). In all the experiments, the buoyant input fluid forms a thin, horizontal compositional boundary layer that is unstable and drains intermittently into the ambient fluid in plumes. The volume ratio of input fluid added to the ambient fluid layer ranged from 1:3 to 1:10. For a given set of Re – U conditions, the different volumetric ratios yielded identical quantitative results.

During the experiments, both still photographs and video were used to record the structure of the convection and the nature of the mixing between the input and ambient fluids. When the experiments were completed and all motion had ceased, density profiles were measured by a combination of direct sampling and a non-invasive optical method (c.f. Jellinek, Kerr and Griffiths, 1998). The results obtained from the two methods indicated that total mass was conserved to within 0.1%.

QUALITATIVE RESULTS

We were concerned primarily with understanding three aspects of the convection and mixing. The first was how the convection evolves from an initial transient phase to a fully-developed flow. The second aspect was the style of the steady-state convection in different Re – U regimes. The third was the relationship between the mechanics of the convective motions and the degree to which the two fluids became mixed.

Small-Re, small-U: Laminar "conveyor-style" stirring

After initiation of an experiment, buoyant input fluid collected in a compositional boundary layer beneath the ambient layer of fluid. The behaviour was consistent with the boundary layer becoming gravitationally unstable at the critical thickness

$$h_c \sim (6.22 V_i \mu_i / g(\rho_a - \rho_i))^{\frac{1}{2}} \tag{7}$$

found theoretically by Kerr (1994), where μ_i is the dynamic viscosity of the input fluid. The first Rayleigh-Taylor instability produced a field of sheet plumes, which had a spacing λ of order πh_c (Kerr, 1994) and a thickness of order h_c. These narrowly-spaced sheet plumes were highly unstable as they ascended and underwent long-wavelength meandering instabilities (c.f. Huppert *et al.*, 1986) that caused them to collide and become entangled. Ambient fluid was folded into contorted plume tops as they rose, and was also carried upwards within meanders, folds, and interstices of entangled plumes. This mechanically entrained ambient fluid, along with ambient fluid that was dragged along the margins of the more viscous sheets, produced a strong but unsteady upward flux of ambient fluid. Returning downflows of ambient fluid dragged buoyant sheets downwards once they reached the top of the ambient fluid layer, forming a "conveyor-style" of circulation on the scale of the ambient fluid layer depth. Continuous overturning and stirring of the two fluids caused the disruption and deformation of sheets, leading to nearly complete mixing.

Small-Re, large-U: Ineffective stirring

When the ambient fluid was much more viscous than the input fluid, the boundary layer grew to a larger critical thickness than in the small-U case before it became unstable. The observed critical thicknesses were consistent with the expression

$$h_c \sim (324)^{\frac{1}{6}} (V_i \mu_i / g(\rho_a - \rho_i))(\mu_a / \mu_i)^{\frac{1}{3}} \tag{8}$$

obtained by Kerr (1994), where μ_a is the dynamic viscosity of the ambient fluid. The first Rayleigh-Taylor instability produced a field of cavity plumes that had a spacing λ of order $(\mu_a / \mu_i)^{1/3}\, \pi h_c$ (c.f. Lister and Kerr, 1989). Cavity plumes are strikingly different to sheets in that they are constructed of a large spherical head and a narrow, axisymmetric umbilical tail (conduit). In these experiments, ascending widely-spaced first generation cavity plumes passed through the ambient fluid and accumulated at the free surface (figure 2). Comparatively thin umbilical conduits that fed the first plume heads remained and acted as low viscosity pathways through which later plume generations drained. A negligible amount of ambient fluid was dragged viscously upwards by rising input fluid, resulting in an imperceptibly weak downflow.

When the flow was fully-developed, the path that input fluid took in traversing the ambient fluid layer

was often complex, and dictated in large part by pre-existing low viscosity conduits which persist for a long time after the rise of individual plumes. The buoyant fluid rose through an elaborate combination of both new Rayleigh-Taylor instabilities and established low viscosity conduits, and then ponded at the top surface. The rising plumes collided with each other and existing conduits, so that plume heads grew larger and conduits supported intermittently very large volume fluxes. The conduits sometimes coalesced and became larger, or pinched off and disappeared.

Several types of long-wavelength instabilities involving conduits were observed when the flow was fully-developed and they probably contributed considerably to the upward flow of ambient fluid caused by viscous drag. Varicose instabilities (cf. Huppert *et al.*, 1986) occurred in some individual conduits that supported short-lived but anomalously high volume fluxes due to the collision and draining of large plume heads. These collisions also led to intermittent traveling waves and other long-wavelength perturbations to conduit walls that augmented the transport of ambient fluid. Weak, meandering instabilities due to the interaction of adjacent, rising plume heads also caused a small increase in the flux of ambient fluid. Despite the presence of these instabilities, the total upward flow was never very large. The resulting very weak circulation did not evolve from the start of an experiment, and so the extent of mixing was very small. Nearly all of the input fluid escaped through the ambient fluid layer to pond as a layer at its top.

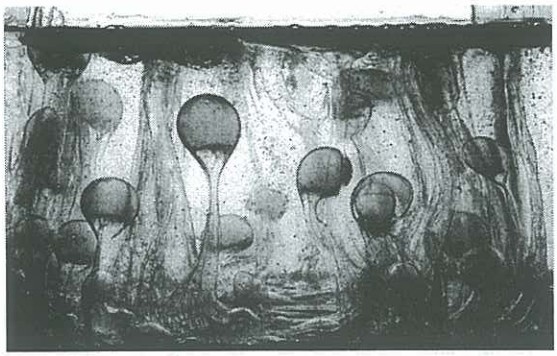

Figure 2 : Photograph taken during an experiment in which $U = 724$ and $Re = 0.33$. Broadly-spaced cavity plumes with large heads ascend through the ambient fluid and pond.

Large-Re, small-U: Turbulent

In this regime, as in the small-*Re*, small-*U* case, the first Rayleigh-Taylor instability produced a field of narrowly-spaced sheet plumes. Individual sheets accelerated from the bottom boundary over a short distance (5-20% of layer depth in this study, depending on plume buoyancy) and were then subject to meandering instabilities, causing them to collide and become entangled. Next, entangled plumes along with entrained ambient fluid coalesced into a fewer number of larger, meandering upwellings that, in turn, became turbulent. The turbulent entrainment of ambient fluid by these upwellings produced a corresponding circulation on the scale of the layer depth. The largest motions associated with the fully-developed turbulent flow swept the bottom boundary layer, entraining and disrupting later plume generations as they rose. Transient perturbations to these largest eddies, resulting from their interaction, caused the abrupt cascade of these motions to very small length scales, resulting in rapid and nearly complete mixing of the two liquids.

Large-Re, large-U: Turbulent mixing

In this regime, a field of cavity plumes rose a short distance from the boundary before meandering instabilities developed on the conduits, causing plume heads to collide with one another and the conduits to become entangled. A large volume of ambient fluid was entrained among entangled conduits and within gaps amidst clusters of plume heads. In most experiments this complicated beginning resulted in the rise of a single, large bundle of interwoven plume heads, conduits, and entrained ambient fluid. The large resultant upward flux of ambient fluid led to equally strong downflows that forced cavity plumes from other regions of the bottom boundary towards this upwelling. This large upwelling collided with the top of the fluid layer, billowed laterally, curled downward, and then penetrated deeply into the layer, entraining a substantial volume of ambient fluid in the process. The flow evolved rapidly to unsteady, laminar overturning on the scale of the ambient layer depth, and then to fully-developed turbulence with the largest eddies equal to the depth of the layer.

As with the large-*Re*, small-*U* experiments, mixing of the two fluids was nearly complete in the large-*Re*, large-*U* regime. Unlike the low-*U* experiments, however, the transition to full turbulence was relatively slow for the same buoyancy flux (occurring over tens of seconds rather than seconds). A feature of interest was that in all large-*Re*, large-*U* experiments cavity plume heads became smaller during the development of the flow. This suggests that a substantial volume of input fluid was stirred into the ambient fluid in the early stages, thereby reducing its viscosity. In one experiment, *U* evolved from 393 to about 10 and caused *Re* to increase from 70.3 to 2740, which is consistent with the transition from unsteady, laminar circulation at the scale of the layer depth to fully-developed turbulence.

QUANTITATIVE RESULTS

A global mixing efficiency

Convection is driven by the release of gravitational potential energy that occurs as buoyant fluid rises. In our experiments this potential energy is released at a fixed rate as kinetic energy. Some of the kinetic energy is used to do the mechanical work of mixing while the remaining kinetic energy is dissipated by viscosity, causing a slight heating of the ambient fluid. The proportion of potential energy used for mixing depends on the interaction between the ambient fluid and the ascending buoyant fluid. In the extreme case of no mixing, buoyant plumes pass through the ambient fluid layer without interaction and collect at the upper boundary. A minimum amount of the initial gravitational potential energy is preserved in the final density profile and so the change in potential energy from the initial to the final states of the system is a maximum. At the opposite extreme of complete mixing, a maximum amount of the initial gravitational potential

energy is preserved in the final density profile, corresponding to a minimum change in the gravitational potential energy of the system over the course of an experiment.

The amount of the available gravitational potential energy used for mixing can be summarized in a single, global quantitative measure of the efficiency of the convective stirring. We first evaluate the potential energy of the final density profile

$$P_f = \int_0^H g(\rho_a - \rho(z))z dz, \qquad (9)$$

where $\rho(z)$ is the density profile at the end of an experiment. The "mixing efficiency" E can then be defined by

$$E = \frac{P_f - P_{min}}{P_{max} - P_{min}}, \qquad (10)$$

where P_{min} is the minimum possible value of the final potential energy (which occurs when there is no mixing), and P_{max} is the maximum possible value of the final potential energy (which occurs when there is complete mixing). In the limits of $P_f = P_{min}$ and $P_f = P_{max}$, $E = 0$ and 1, respectively.

Dependence of mixing efficiency on *Re* and *U*

Quantitative results for the dependence of the mixing efficiency E on Re and U are presented in the form of a contour map in figure 4. Measured density profiles corresponding to certain mixing efficiencies are shown in figure 3. The most intuitive result was that high mixing efficiencies ($E > 0.9$) occurred when the convection was turbulent ($Re > 100$). The most striking discovery was that *equally large mixing efficiencies were found in all Re regimes when U < 1;* i.e. when the viscosity of the ambient fluid was less than that of the input fluid. In particular, unsteady laminar convection resulted in nearly complete mixing when $Re < 1$ and $U < 1$. The critical feature in all high E regimes was that for a given buoyancy flux, *rising plumes entrained a large volume of ambient fluid which, in turn, led to a strong large-scale circulation that disrupted and stretched plumes to very small length scales, causing extensive mixing.* Low mixing efficiencies ($E < 0.1$), on the other hand, were observed only when $Re < 1$ and $U > 200$. The main characteristic of this regime was that a very small total upward flow of ambient fluid, due predominantly to viscous drag, produced no large-scale circulation, and hence input fluid passed through the ambient fluid layer and ponded. The very low (but non-zero) efficiencies determined for this regime probably reflect that in the absence of circulation, most of the mixing occurred as a result of the diffusive contamination of plumes as they rose through the ambient fluid.

ACKNOWLEDGEMENTS

This research was supported by an ANU Ph.D. Scholarship and an Overseas Postgraduate Research Scholarship (AMJ), and an Australian Research Council Fellowship (RCK).

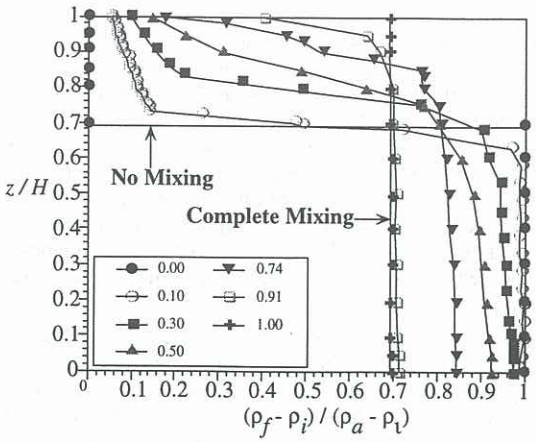

Figure 3 : The mixing efficiency expressed in terms of normalized density profiles measured at the end of certain experiments. The efficiency is reflected in both the shape of the profile and by the minimum and maximum densities recorded.

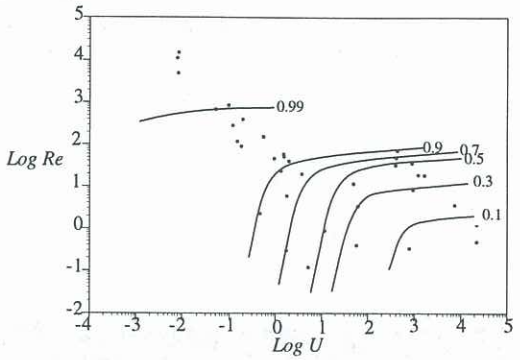

Figure 4 : A contour map showing the experimental mixing efficiencies as a function of *Re* and *U*.

REFERENCES

HUPPERT, H.E., SPARKS, R.S.J., WHITEHEAD, J.A. and HALLWORTH, M.A., "Replenishment of magma chambers by light inputs", *J. Geophys. Res.*, **91**, 6113-6122, 1986.

JELLINEK, A.M., KERR, R.C. and GRIFFITHS, R.W., "Mixing and compositional layering produced by natural convection. Part 1. The experiments, and their application to the Earth's core and mantle", *J. Geophys. Res.* (submitted), 1998.

KERR, R.C., "Melting driven by vigorous compositional convection", *J. Fluid Mech.*, **280**, 255-285, 1994.

KRAICHNAN, R.H., "Mixing-length analysis of turbulent thermal convection at arbitrary Prandtl numbers", *Phys. Fluids*, **5**, 1374-1389, 1962.

LISTER, J.R. and KERR, R.C., "The effect of geometry on the gravitational instability of a buoyant region of viscous fluid", *J. Fluid Mech.*, **202**, 577-594, 1989.

WHITEHEAD, J.A. and LUTHER, D.S., "Dynamics of laboratory diapir and plume models", *J. Geophys. Res.*, **80**, 705-717, 1975.